Journal of Alloys and Compounds 505 (2010) 183–187

Contents lists available at ScienceDirect

Journal of Alloys and Compounds

journal homepage: www.elsevier.com/locate/jallcom

Hydrogen absorption in as-cast bcc single-phase Ti–Al–Nb alloys

A.M. Patselov[a,*], V.V. Rybin[b], B.A. Greenberg[a], N.V. Mushnikov[a]

[a] Institute of Metal Physics, Ural Branch of RAS, 18 S. Kovalevskaya Str., 620990 Ekaterinburg, Russia
[b] Central Research Institute of Structural Materials, St-Petersburg, Russia

ARTICLE INFO

Article history:
Received 6 March 2009
Received in revised form 8 June 2010
Accepted 10 June 2010
Available online 16 June 2010

Keywords:
Hydrogen absorbing materials
Gas–solid reactions
Diffusion
Kinetics
Phase transitions

ABSTRACT

In this article, hydrogen absorption properties of bcc single-phased as-cast Ti–Al–Nb alloys near pseudo-binary section at about 50 at.% of Ti are considered. Possible reasons of enhancing hydrogen capacity with the increasing of Nb content from ~34 to ~42 at.% and decreasing Al content from ~13 to ~6 at.% are discussed. The alloys and corresponding hydrides have been characterized by X-ray diffraction. Ti–6 at.% Al–42 at.% Nb is found to absorb maximum hydrogen H/M = 1.88 (~2.81 wt.%) to form a hydride at 500 °C temperature and 1.2 MPa. Beneficial effect of mild cold rolling deformation on hydrogen capacity is noted. All the studied compositions demonstrate good kinetics and absorb hydrogen quickly, within 20–30 min after activation.

1. Introduction

Ti–Al–Nb system represents a numerous group of alloys and intermetallic compounds. Alloys with relatively low additions of Nb mainly based on α_2 (hcp crystal lattice) phase and being in the ordered state consist of the orthorhombic O-phase and/or ordered B2-phase (bcc lattice). They have become the focus of attention as potential high temperature structural materials for aircraft engine and airframe applications due to their attractive high specific strength and fracture toughness [1]. However, several years ago a few publications about hydrogen storage properties of such class of Ti–Al–Nb alloys appeared [2–5]. Well-established knowledge of the nature of phase equilibria and transformations in the above system [6–9] allows for systematic control over different microstructures. Using Ti–22Al–27Nb as a base alloy hydrogen absorption/desorption behavior in B2 ordered single-phase state before and after deformation [2], multiphase effects [3] and beneficial effect of orthorhombic O-phase on the hydrogen absorption [4] were studied. Authors of the above articles supposed that bcc-based phases of Ti–Al–Nb system occurring by adding Nb to Ti_3Al may have a greater hydrogen absorption capacity since loosely packed bcc-based structures are usually superior to closely packed fcc- and hcp-based structures in hydrogen absorption. The maximum hydrogen capacity of the alloys investigated [2–5] does not exceed 2.0 wt.%. It should be noted, however, that all samples in the above studies were subjected to high temperature treatment in order to receive different single or multiphase microstructures before hydrogenation.

Different from the authors who were quoted above we decided to increase the range of Ti–Al–Nb system alloys in order to assess a potential influence of the chemical composition on hydrogen capacity of these alloys. We also intended to check on the effect of the influence of mild deformation on the hydrogen capacity of our alloys compositions. We studied alloys with 34–42 at.% Nb and 6–13 at.% Al, Ti content being about 50 at.%. Since the preliminary studies (see Fig. 5 in [10]) as well as our unpublished results indicate that the hydrogen capacity of the as-cast specimens exceeds that of the homogenized specimens (solution treatment at 1360 °C, 24–36 h) by ~1.5 we used only as-cast specimens in our further work. To avoid possible influence of such parameters as multiphase effects, degree of ordering, etc. on hydrogen capacity, we took into account state diagrams published elsewhere. As a possible guide we used the pseudo-binary section of the Ti–Al–Nb system at 50 at.% Ti taken from [11] which, in its turn was taken from Bendersky et al. [12] with data sourced from references [7,13] (see Fig. 15 from [11]). Composition-induced disordering of the bcc phase was observed in several Ti–Al–Nb alloys and higher Al contents favor the ordered B2 structure [7,12,14]. According to [11], for Ti–15Al–33Nb the ordered B2 structure was not detected in the as-processed (899 °C) and solution-treated conditions. The authors of [11] reported that the B2-phase had not expected as the bcc composition could not contain more than 15 at.% Al and less than 33 at.% Nb and thus the temperature range of stable B2-containing microstructures was significantly reduced for lower Al-containing and higher Nb-containing alloys. The above explain our choice of composition range for as-cast

* Corresponding author. Tel.: +7 343 378 3829.
E-mail address: patselov@imp.uran.ru (A.M. Patselov).

0925-8388/$ – see front matter © 2010 Elsevier B.V. All rights reserved.
doi:10.1016/j.jallcom.2010.06.026

alloys, where instead of ordered B2-phase only disordered β-solid solution expected.

2. Experimental

The purities of the raw materials, niobium, titanium and aluminum were 99.9, 99.95 and 99.995 wt.%, respectively. The ternary alloys with nominal compositions 6–13 at.% Al, 34–42 at.% Nb, balance – Ti were prepared into rod shaped ingots of about 30 or 50 g in a vacuum arc-melt furnace under purified helium atmosphere. To achieve macro-homogeneity of composition, the ingots were remelted 3–4 times before crystallization into copper ingot mould. The specimens were variously shaped, the thickness being about 1.2–1.3 mm thick cut of the rod by an electrodischarge machine, with follow up chemical polishing to remove machine damage and surface contamination.

Each alloy was hydrogenated to the maximum storage capacity using high pressure Sieverts apparatus. Hydrogenation was carried out with high-purity hydrogen gas obtained by decomposition of $LaNi_5H_x$ hydride. The samples were activated by vacuum heat treatment before exposure to hydrogen. In each activation process, the samples were evacuated to the pressure of 0.1 Pa and heated at 500 °C for 15–30 min. The variations of the pressure versus time were recorded. Hydrogen storage capacity was measured by weight method.

The macro- and microstructures were examined using an optical microscope (OM) and scanning electron microscope (SEM) equipped with an energy dispersive X-ray spectrometer (EDS) to determine chemical composition of the samples. The lattice parameters of the samples before hydrogen absorption were detected by X-ray diffraction (XRD) analysis using Cu Kα radiation. The dislocation structure of as-cast alloys was studied in a JEM200CX transmission electron microscope (TEM).

3. Results and discussion

The results of hydrogenation of as-cast alloys specimens are shown in Table 1. The order of presenting the results follows the variations in the composition: Nb content increasing gradually and Al content decreasing. It is obvious that such tendency leads to enhancement of the hydrogen capacity within the range of the tested compositions. But before proceeding to discussing the obtained results, characteristic features of the metastable β-solid solutions, their structure before hydrogenation as well as kinetics of the hydrogenation process proper should be reviewed.

Table 1
Hydrogen absorption capacity in H/M units.

Source	Al[a]	Nb	Ti	H/M
Data of [17]	14.8	25.9	Bal.	0.74
Our data	13.4	34.2	Bal.	0.83
Our data	10.4	36.9	Bal.	1.00
Our data	10.6	39.9	Bal.	1.42
Our data	06.1	39.8	Bal.	1.58
Our data	06.1	41.9	Bal.	1.88

[a] Composition of alloys in at.%.

Most of the commercial β-titanium alloys are metastable with regard to the β-phase. Typical (TEM) microstructure of the metastable as-cast alloy is presented in Fig. 1a. In the real experiment metastability is determined by occurrence of diffusion lines in between β-phase reflections on TEM microdiffraction image (insertion in Fig. 1a). Metastability allows for adjustment of the mechanical properties with respect to the specific applications by means of a two-step heat treatment. In a first step usually a solution

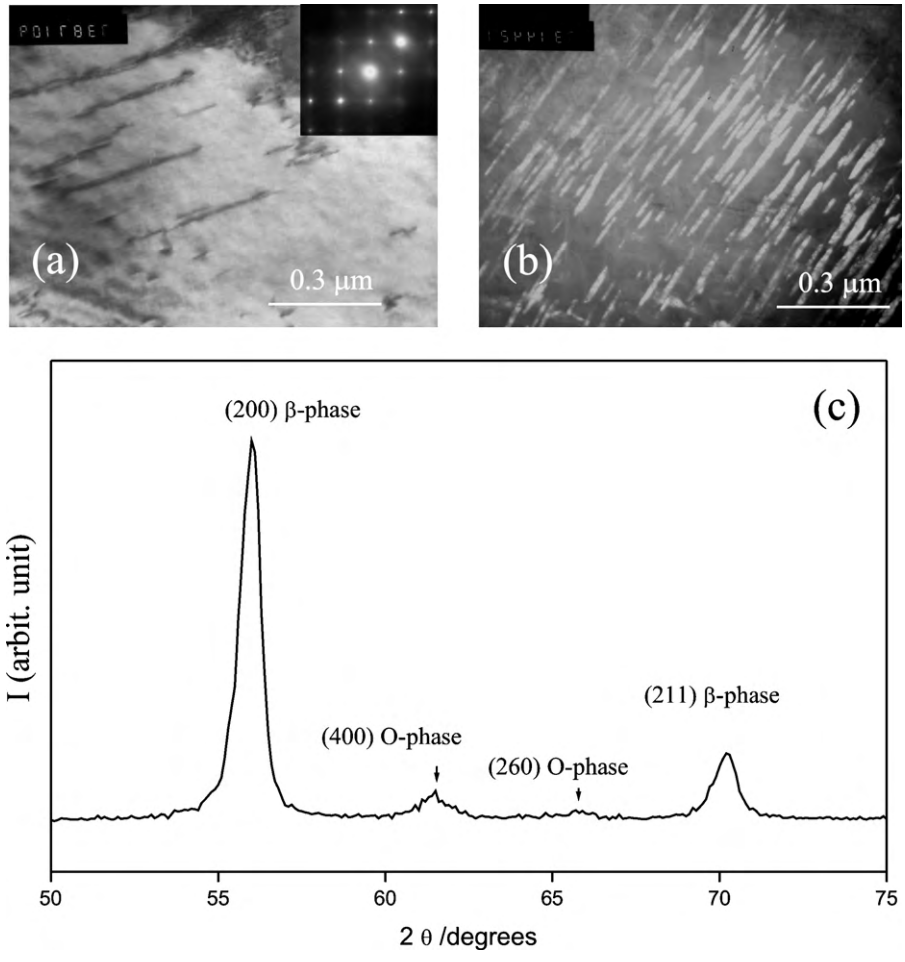

Fig. 1. Microstructure of the Ti–11Al–40Nb: (a) as-cast, (b) after aging and (c) fragment of X-ray diffraction pattern for aging sample.

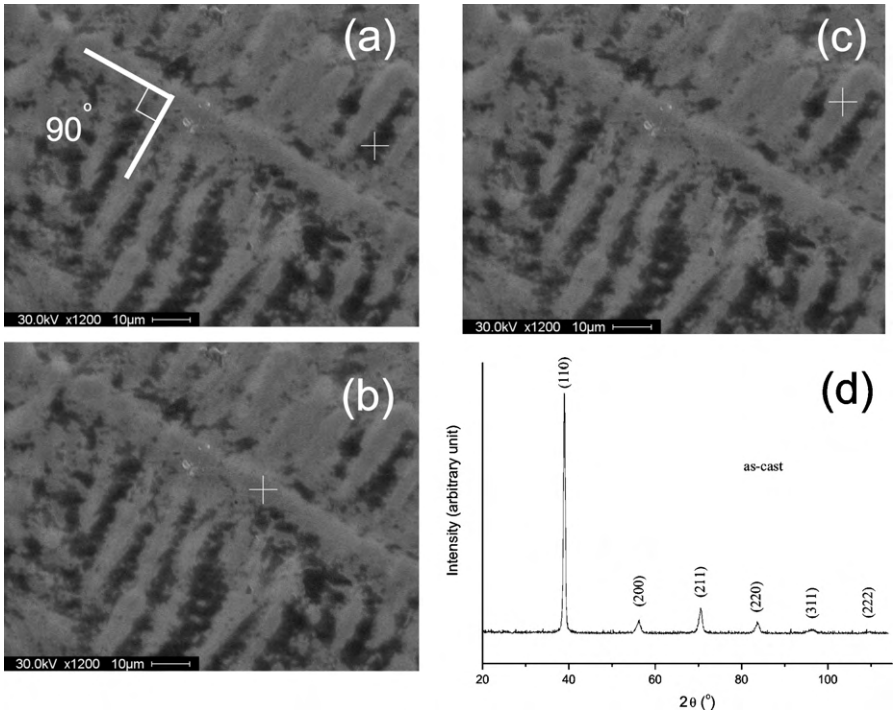

Fig. 2. SEM micrographs of cross-sections with dendrite structures (analyzed positions marked by '+' sign, a, b, and c) and X-ray diffraction pattern for Ti–10Al–40Nb (d).

annealing above or slightly below the β-transus[1] is carried out. It is typical of this type of alloy that the β-phase is not transformed during quenching to room temperature. The final strength of the material can be adjusted by aging at intermediate temperature (typically between 350 and 600 °C) and results from the precipitation of fine α or ω needles or plates embedded in the β matrix. For some triple Ti–Al–Nb alloys with certain Al/Nb ratio at fixed titanium concentration the precipitation of orthorhombic O-phase is possible [7–9]. Electron-microscopic bright-field image in Fig. 1b as well as X-ray diffraction pattern fragment in Fig. 1c confirming occurrence of O-phase precipitation are examples of such structure which resulted from the above two-step treatment. The second step in the above example was aging at 650 °C during 5 h with subsequent furnace cooling. According to [15] aluminum additions make it possible to avoid ω-phase precipitations in Ti–Nb solid solutions. These are metastable as-cast alloys with corresponding aluminum doping level as well as accelerated procedure of hydrogenation that help avoiding second phase precipitation.

Structures of as-cast samples before hydrogen absorption experiments have dendrite character. Fig. 2a–c illustrates the ~90° angle between the dendrite arms, which is a characteristic feature of the cubic phase. It can be assumed that enhanced hydrogen capacity of the as-cast alloys (in comparison with homogenized specimens) could be accounted for by internal surfaces between dendrites and interdendritic space. Another reason may be existence of β-phases of different composition inside dendrites and inside interdendritic space as well as better absorption of hydrogen by one such phases. To determine the controlling factor changes in Ti and Nb content in dendrite arms and interdendritic space had to be established using EDS system of scanning electron microscope. Such measurements were performed for the Ti–9.65 at.% Al–40.41 at.% Nb sample (Ti–10Al–40Nb). According to the EDS analysis results which are shown in Table 2, niobium was accumulated in the center of the dendrite arms whereas the interdendritic regions were enriched with Ti. Positions for EDS analysis are marked by plus sign in Fig. 2a–c. The X-ray analysis also confirms the appearance of fundamental reflections of the disordered base-centered cubic β-phase of as-cast samples for all the compositions described here (Fig. 2d).

Table 2
EDS analysis for distribution of base elements in dendrites structures.

Position	Ti[a]	Nb
Average per volume	49.94	40.41
I order dendrites arms	47.50	43.00
II order dendrites arms	46.90	43.30
Interdendritic regions	52.96	37.66

[a] Composition in at.%.

Fig. 3 shows kinetics curves of some investigated alloys. It is obvious that all the bulk samples studied absorb hydrogen quickly (within 20–30 min) after activation. After hydrogen absorption they transform into coarse powder with the average size of particles 0.1–1.0 mm. Some alloys were machined into chip scrap before hydrogenation to see what will happen with the kinetics

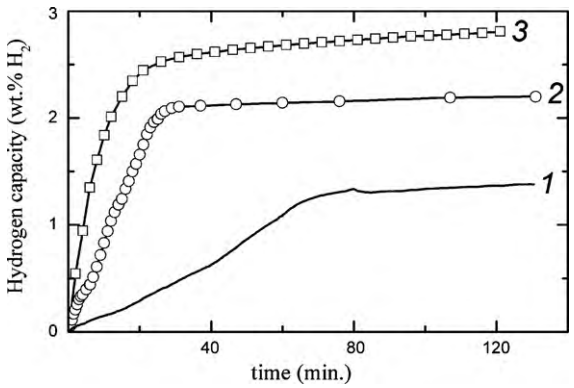

Fig. 3. Kinetics curves of hydrogen absorption: 1 – Ti–13Al–34Nb; 2 – Ti–11Al–40Nb; 3 – Ti–6Al–42Nb

[1] β-Transus is the α–β transformation temperature in titanium alloys.

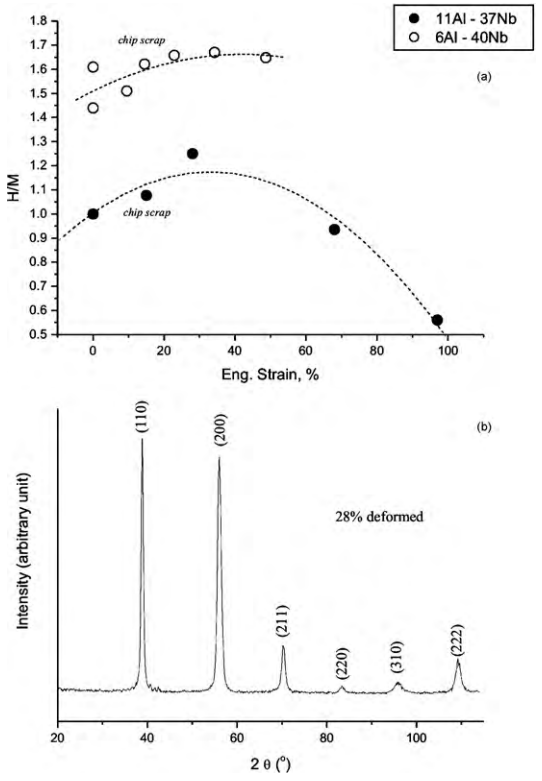

Fig. 4. Effect of deformation on hydrogen capacity of cast disordered bcc alloys for two sets of composition (a) and X-ray diffraction pattern for cold rolled Ti–10Al–36Nb (b).

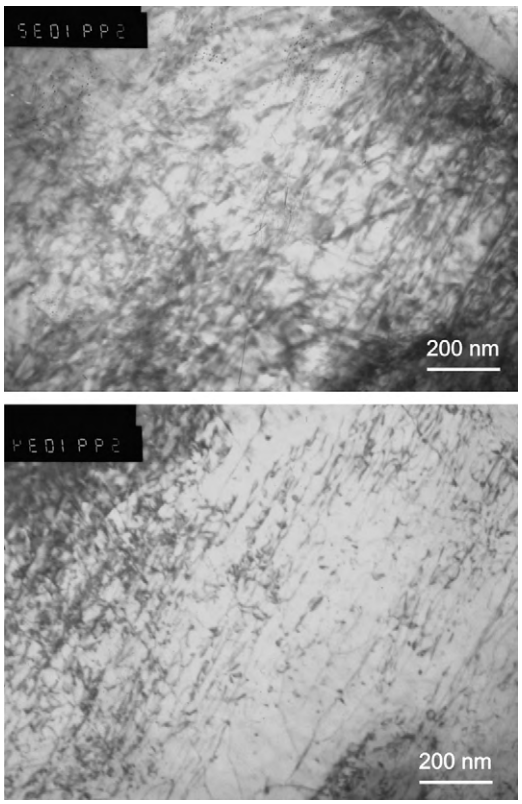

Fig. 5. TEM microstructures of specimens before hydrogen absorption: high-density of long-distanced, jogged, twisted dislocations, tangled configurations.

of hydrogenation. As a result the time needed for accomplishing the hydrogenation process was about 3–5 min. Probably it is due to a larger surface of chip scrap in comparison with the relatively thick bulk samples as well as shorter hydrogen diffusion paths. The hydrogenation process begins with the formation of interstitial solid solution of hydrogen atoms in bcc lattice of the Ti–Al–Nb alloy and finishes with the hydride phase. It is known [16] that pressure increasing, hydrogen solubility in metals grows and when it reaches the ultimate value corresponding with the beginning of the second, higher hydrogen phase appearance the plateau of equal pressures forms on the solubility isotherms. Pressure remains constant until the two-phase region is replaced by a single-phase one with hydrogen content higher than in solid solution. But neither of the examined compositions showed the above plateau. The absence of plateau does not allow calculating the enthalpy of the hydride phase because Van't Hoff equation requires the plateau pressure value. Also, the same absence of plateau was noted in [17] for Ti–14.8 at.% Al–25.9 at.% Nb alloy on pressure-composition isotherms at 500 °C. According to [4] Ti–22Al–27Nb alloy hydride formation enthalpy is 30–45 kJ/mol H_2. It should be noted that the process accelerates with Nb content increasing and Al content decreasing in all specimens within the examined composition range.

In [2] it was shown that mild deformation improves both absorption and desorption properties of B2 single-phased Ti–22Al–27Nb alloy. The results of our studies into the effect of deformation on hydrogen capacity of cast disordered bcc alloys are presented in Fig. 4a. The graph shows two series of experimental points. The first set relates to the results of measurements of hydrogen capacity in solid solutions with aluminum content from 10.4 to 10.9 at.%, niobium from 36.4 to 41.1 at.%, balance – titanium. The second series contains data on hydrogen capacity for alloys with lower concentration of aluminum (from 5.0 to 7.4 at.%), niobium (from 39.4 to 40.5 at.%), balance – titanium. Deformation for points in both series, designated by the word "chip scrap", was determined by chip scrap shrinkage calculations, and according to these, it does not exceed 15%. The penultimate (last but one) point in the series "11–37" was taken for a sample subjected to hot rolling in a stainless steel can at 950 °C for several reductions. We allowed ourselves to include this result into the series because the cast structure in this treatment was preserved and in terms of structure this specimen did not differ from the samples treated by cold rolling. According to [7], only the total strain in three units of true logarithmic strain is able to break the cast structure of disordered Ti–Al–Nb solid solutions. According to the plot for alloys with lower

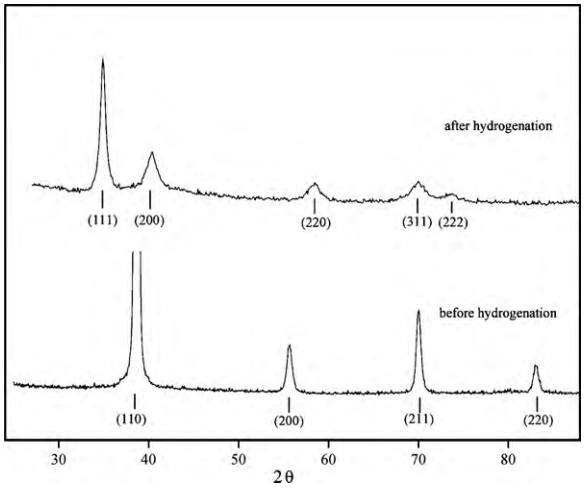

Fig. 6. Diffraction pattern of the Ti–6Al–41Nb samples: (a) before and (b) after hydrogenation.

aluminum content (marked on the plot as "6–40" series), besides rising and drop sections of hydrogen capacity, there is a relatively straight section for a range of strains from about 20 to 50%. The same plot section can be identified for the series with high aluminum content, denoted as "11–37"series. If not to take into account the scatter of (widely varying) data for the undeformed state, then a tendency is clearly observed. According to X-ray diffraction studies no phase changes are observed, only rearrangement of integral intensities due to texture of rolling is visible (see Fig. 4b). It is seen that 28% (engineering strain) deformation by cold rolling resulted in about quarter increase of hydrogen capacity in comparison with undeformed alloy of the same composition. Another piece of the above alloy was cold rolled to 97% (engineering strain) deformation to see what will happen with hydrogen capacity. The resulting value is 0.56 H/M of hydrogen in the first hydrogenation cycle. The authors of [2] proposed an explanation that beneficial effect of mild deformation on the hydrogen absorption behavior should be closely associated with the structure of well-aligned and uniformly distributed screw dislocations. In work [2] term "mild deformation" was applied to samples that were subjected to 5 and 10.5% thickness reduction deformation. According to TEM investigations of [2] corresponding microstructures of the above samples do contain a lot of well-aligned and uniformly distributed dislocations. The recalculating 5–10% thickness reductions into true effective deformation will give us the assurance that we indeed deal with initial stages of deformation and the occurrence of aligned and distributed dislocations is characteristic feature of the above stage. As for the 28% deformed cold rolled sample it already demonstrates a lot of curvilinear intersect dislocations including tangled configurations in TEM microstructures (see Fig. 5). Nevertheless, we have about 25% increases in hydrogen capacity for deformed samples. There seems to exist a more complex explanation of beneficial effect of deformation on the hydrogen absorption behavior but additional work on this phenomenon in a future independent investigation is required. Comparison of the data on deformation behavior with structural changes requires a lot of illustrative information—TEM, SEM images, diffraction patterns. We think that it will be more correct to present such comparison in a separate article.

The hydrogenation process begins with the formation of a (Ti–Al–Nb)–hydrogen solid solution with the follow up formation of the hydride phase. X-ray diffraction patterns for Ti–6Al–42Nb alloy before and after hydrogenation are shown in Fig. 6 as an example. The initial single-phase has bcc structure with the lattice parameter $a = 0.329$ nm. As for the phase which appears after the first cycle of hydrogen absorption its diffraction pattern can be described as a fcc lattice with the parameter $a = 0.447$ nm.

The received hydrogen capacities are presented in the right hand column of Table 1 for as-cast alloys and in Fig. 4a for as-cast and deformed alloys. These values vary within wide range from 0.56 to 1.88 H/M depending on both basic elements content and deformation treatment. It is obvious that the investigated as-cast alloys have the same and only single metastable β-phase before hydrogen absorption. At the same time they demonstrated more than 100% difference in a maximum of attainable hydrogen capacity for them. A general tendency in such a row of as-cast alloys is the rise of hydrogen capacity at increasing of niobium content and decreasing of aluminum content. Taking into account that both Ti and Nb, unlike Al, are hydride forming elements, we come to the conclusion that increment of hydride forming elements in solid solution leads to corresponding enhancing of hydrogen capacity and vice versa. It is exactly the situation we observe in Table 1. The increase of bcc crystal lattice parameter as well as microporosity of as-cast structure giving some additional looseness and contributing to enhancing of hydrogen absorption capacity should not be neglected either.

4. Conclusion

In this work, a general tendency in improving the hydrogen absorption capacity after the first hydrogenation cycle with the increasing Nb content in the range of 34–42 at.% is shown for the as-cast bcc disordered Ti–Al–Nb alloys. Ti–6 at.% Al–42 at.% Nb is found to absorb maximum hydrogen H/M = 1.88 (2.81 wt.%) to form a hydride at 500 °C temperature and 1.2 MPa. It should be noted, however, that the above tendency is limited by phase stability of the disordered bcc β-solid solution within the temperature range of hydrogen treatment as well as duration of activation process. Also, beneficial effect of certain extent of deformation on hydrogen capacity is confirmed. However, additional independent work is needed to clarify this phenomenon.

Acknowledgments

The authors thank Prof. Goltsov V.A. for his incentive discussions and useful suggestions during the preparation of this manuscript. Use of electron microscope facilities at the Center for electron microscopy analysis in the Institute of Metal Physics (Ural Branch of Russian Academy of Sciences) is acknowledged. This study was financially supported under the program "National Technological Basis" (Agreement No. 51/07/945-2007).

References

[1] A.K. Gogia, T.K. Nandy, D. Banerjee, T. Carisey, J.L. Strudel, J.M. Franchet, Intermetallics 6 (1998) 741–748.
[2] L.T. Zhang, K. Ito, V.K. Vasudevan, M. Yamaguchi, Acta Mater. 49 (2001) 751–758.
[3] K. Ito, L.T. Zhang, V.K. Vasudevan, M. Yamaguchi, Acta Mater. 49 (2001) 963–972.
[4] L.T. Zhang, K. Ito, V.K. Vasudevan, M. Yamaguchi, Intermetallics 9 (2001) 1045–1052.
[5] L.T. Zhang, K. Ito, H. Inui, V.K. Vasudevan, M. Yamaguchi, Acta Mater. 51 (2003) 781–788.
[6] D. Banerjee, A.K. Gogia, T.K. Nandy, K. Muraleedharan, R.S. Mishra, in: R. Darolia, J.J. Lewandowski, C.T. Liu, P.L. Martin, D.B. Miracle, M.V. Nathal (Eds.), Structural Intermetallics, TMS, Warrendale, PA, 1993, pp. 19–33.
[7] C.J. Boehlert, B.S. Majumdar, V. Seetharaman, D.B. Miracle, Metall. Mater. Trans. A 30A (1999) 2305–2323.
[8] C.J. Boehlert, D.B. Miracle, Metall. Mater. Trans. A 30A (1999) 2349–2367.
[9] C.J. Boehlert, Metall. Mater. Trans. A 32A (2001) 1977–1988.
[10] K. Ito, Y. Okabe, L.T. Zhang, M. Yamaguchi, Acta Mater. 50 (2002) 4901–4912.
[11] C.J. Cowen, C.J. Boehlert, Philos. Mag. 86 (1) (2006) 99–124.
[12] L.A. Bendersky, W.J. Boettinger, A. Roytburd, Acta Metall. Mater. 39 (1991) 1959–1969.
[13] C.J. Cowen, C.J. Boehlert, Intermetallics 14 (4) (2006) 412–422.
[14] H.T. Kestner-Weycamp, C.W. Ward, T.F. Broderick, M.J. Kaufman, Scripta Metall. 23 (10) (1989) 1697–1702.
[15] V.A. Vozilkin, T.L. Trenogina, S.B. Volkova, Phys. Met. Metallogr. 5 (1992) 493–497.
[16] G. Alefeld, J. Völkl (Eds.), Hydrogen in Metals, vol. 2: Application-oriented Properties, Springer, Berlin, Heidelberg, 1978.
[17] B. Dutta, T. Keller, M. Rettenmayr, U. Jantsch, D.F. Lupton, Mater. Sci. Eng. A 382 (2004) 57–63.